Enthalpy and Heat Capacity of Cs–Pb Alloys in Solid and Liquid States

Andrei R. Khairulin[1] · Sergei V. Stankus[1]

Abstract

The enthalpy of Cs–Pb system alloys containing 40, 50, 60, and 66.67 at.% Pb have been measured and heat capacity have been determined using high-temperature drop calorimetry method over a temperature range 430–1075 K covering solid and liquid phases. For all alloys, recommended temperature dependences of the studied properties have been developed as well as the enthalpy changes on phase transitions and the liquidus temperature have been determined. The concentration dependence of the heat capacity of Cs–Pb liquid alloys at different temperatures has been constructed, at which the pronounced maximum is observed at a content of 50 at.% Pb. A significant excess of the heat capacity of the studied melts over additive values is revealed. It is shown that the results obtained are consistent with the assumptions in the literature about the formation of structural units with a partially ionic character of interatomic interaction in melts of the Cs–Pb system.

Keywords Cesium–lead alloys · Drop calorimetry · Enthalpy · Heat capacity · Melting · Solid and liquid states · Solid-phase transition

1 Introduction

Alloys of alkali metals with lead belong to a rather rare and poorly investigated class of substances in which, according to the modern concepts, melts are prone to complication of the short-range order structure, namely, to the formation of ionic interatomic bonds in their structure. This behavior is explained by the fact that lead, which has a higher electronegativity than alkali metals, acts as an oxidizing agent. It is considered that in liquid cesium–lead system alloys, tetrahedral complexes Cs_4Pb_4 are formed, in which lead anions are surrounded by cesium cations [1].

✉ Andrei R. Khairulin
rainjke95@yandex.ru

1   Kutateladze Institute of Thermophysics, Siberian Branch of the Russian Academy of Sciences, 1
     Lavrentyev Avenue, 630090 Novosibirsk, Russia

This assumption is indirectly confirmed by researching structure-sensitive properties. Thus, on the concentration dependence of the electrical resistance of the liquid Cs–Pb system, the pronounced maximum is observed at a content of 50 at.% Pb [2], and the relative excess molar volume, in turn, has its minimum at the same concentration [3]. With raising temperature, complexes dissociate, which leads to the extremes on the concentration dependences of such properties as the volumetric coefficient of thermal expansion [3] and the temperature coefficient of resistance [2]. Studies of the structure of liquid alloys of alkali metals with lead also brought a number of indirect proofs of the possibility of ordered structural units in their composition. Neutron diffraction studies of Na–Pb, K–Pb, Rb–Pb, Cs–Pb alloys [4] showed that the radial distribution function in the liquid state has a peak that corresponds to the interatomic distance in Pb tetrahedra in the solid state. Simulation using molecular dynamics methods [5] also shows the possibility of the formation of complexes in the form of lead tetrahedrons in the melts structure of the Cs–Pb system.

The presence of structural features is also reflected in the anomalously high heat capacity of liquid equiatomic Cs–Pb alloy, which quickly decreases in a short temperature range [6]. Unfortunately, no data on the enthalpy and heat capacity of liquid Cs–Pb system alloys of other compositions were found in the literature. At the same time, the results of measuring the caloric properties of the Cs–Pb system alloys in a wide range of temperatures and concentrations could make a significant contribution to the experimental database necessary for the development of the theory of the so-called ion-metal melts.

The phase diagram of the cesium–lead system was apparently obtained in a single work and was based on the measurements of the electrical resistance of alloys [2]. Subsequently, the caloric properties of the equiatomic Cs–Pb alloy [6] and the density of 8 alloys in the liquid state [3] were measured, which clarified the position of the liquidus line. The data from [3] and [6] are in good agreement with each other, but differ significantly from the results of [2].

In connection with the above, the purpose of this work is to obtain new experimental data on the caloric properties of the cesium–lead system in solid and liquid states, as well as to clarify the temperatures of phase transitions in this system.

2 Experimental Details

Four alloys of the Cs–Pb system containing 40, 50, 60, and 66.67 at.% Pb were studied (Table 1). The raw metals contained 99.94 wt% (99.932 at.%) cesium and 99.992 wt% (99.975 at.%) lead. The stated purity is based on metallic impurities. Main impurity elements in cesium are alkali metals while in lead it is bismuth. Sample preparation took place in a glove box in an atmosphere of pure argon (99.992 vol%). The concentration of components was determined by weighting with electronic scales installed in the box. The uncertainty of composition did not exceed 0.02 at.%. The purity of the components was not taken into account when assessing the error in determining the composition—it was based only on the weighing error. As measuring cells, we used stainless steel (the analog of AISI-321) ampoules

Table 1 Studied samples of Cs–Pb system alloys

Sample	Content of Pb, at.%	Sample mass, g	Molar mass of alloy, g/mole
Cs33Pb67	66.67	50.831	182.436
Cs40Pb60	60.00	45.186	177.480
Cs50Pb50	50.00	38.304	170.049
Cs60Pb40	40.00	32.771	162.620

sealed by electric arc welding also inside the glove box. The ampoules had the shape of a truncated cone with a lid, into which a thin-walled sleeve was welded for inserting a thermocouple and suspending the ampoule. The thermocouple (type S) was verified by the solidification points of pure tin, lead, aluminum, and copper in the calorimeter furnace in the sample cooling mode at a rate of 2–3 K min^{-1}. Based on the results of these experiments, the temperature in all subsequent experiments was adjusted accordingly.

Thermal analysis of the alloys was carried out in a calorimeter furnace on ampoules prepared for enthalpy studies. The measurement procedure consisted of heating the ampoules to 1073 K, isothermal holding for 1–2 h, and cooling at a constant rate of 10–15 K min^{-1} to a temperature 50–60 K higher than the liquidus temperature and a rate of 1–3 K min^{-1} at a lower temperature. This thermal regime was chosen based on the experiments [3], where the homogeneity of the melts was controlled by scanning samples with a beam of gamma rays in height.

The main experiments were carried out using the isothermal drop calorimeter, the design of which and the method of processing primary data are described in detail in [7–9]. Below is a brief description of the equipment.

The calorimetric unit is a massive copper cylinder (24 kg) with a blind conical hole for the ampoule, a copper resistance thermometer (100 Ohm) wound onto its surface, a built-in electric heater for calibrating the block, and a copper cover that opens and closes the conical hole only for ampoule falling time (Fig. 1). The block is hermetically suspended on a thin-walled pipe to the upper flange of the isothermal shell, on which a second copper cover is installed, operating synchronously with the first. The space between the block and the shell is evacuated to a pressure of 0.1 mPa. The constant temperature of the calorimetric block shell is maintained by a liquid thermostat with long-term instability of no more than 0.001 K.

Directly above the calorimetric block there is an electric furnace with a tubular molybdenum heater, an equalizing molybdenum block, two guard heaters, a system of thermoradiation shields, and also evacuation and argon filling systems. On the upper flange of the furnace there is a lock chamber for installing the ampoule on a movable rod with a thermocouple, which moves the ampoule into the furnace. The ampoule holder is a mechanical lock that is opened by an electromagnet. The thermocouple enters the protective sleeve of the ampoule, which slides off from thermocouple when the lock is opened.

The ampoule drop procedure is automatic. The covers and the mechanical lock open after swinging the water-cooled shield and close after the flight sensor is
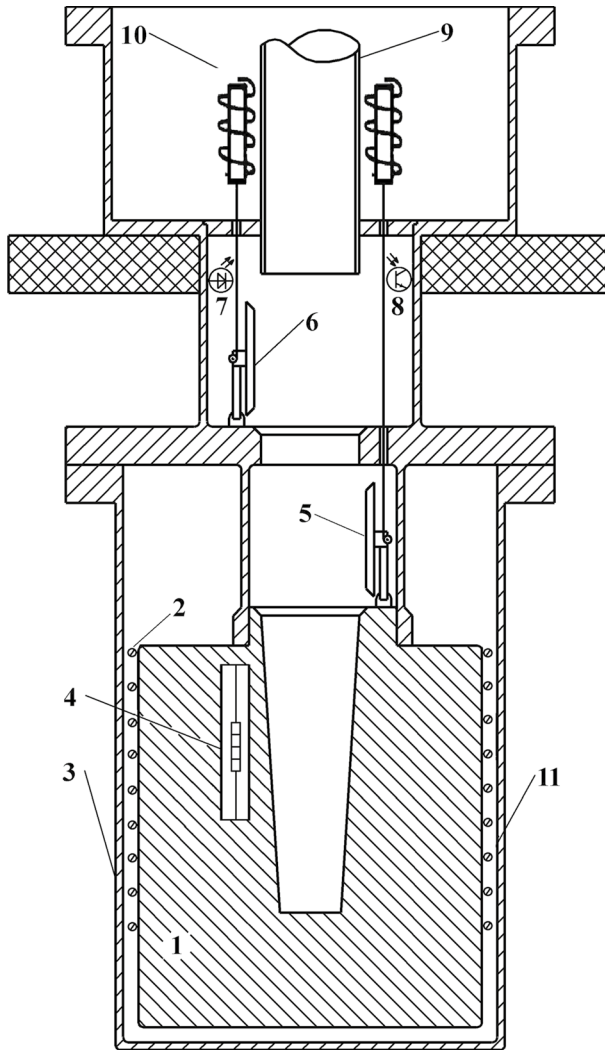
Fig. 1 Calorimetric unit. *1*—copper block; *2*—copper resistance thermometer; *3*—isothermal shell; *4*—calibration heater; *5*, *6*—copper covers; *7*—light-emitting diode; *8*—phototransistor; *9*—guide pipe; *10*—solenoid; *11*—vacuum gap

triggered (7, 8 in Fig. 1). It cuts to a minimum the time when the calorimeter covers are opened, and also make it identical for all experiments. In this case, the error associated with heat loss from the ampoule in the main and calibration experiments is mutually compensated.

Before carrying out the main experiments, measurements of the thermal equivalent and heat transfer coefficient of the calorimetric block were made, as well as the temperature dependence of the mass enthalpy of the empty ampoule was defined.

Table 2 Phase transition temperatures and enthalpy change on phase transitions

	Cs33Pb67	Cs40Pb60	Cs50Pb50	Cs60Pb40
T_L, K	839 ± 1.5	876.7 ± 1.5	918.3 ± 1.5	$802* \pm 3$
ΔT_{UR}, K	0	0	$0.6 - 1.8$	$10\text{—}16$
ΔH_f, J/mol	9150 ± 45	6711 ± 160	3610 ± 54	–
T_t, K	834 ± 1.5	–	$871* \pm 3$	–
ΔT_{UR}, K	0.03	–	$11\text{—}23$	–
ΔH_t, J/mol	–	–	6098 ± 10	–

*Extrapolation to zero subcooling. Enthalpy changes on phase transformations are determined using approximation equations at T_L and T_t. For enthalpy, the standard error of type A is given

Fig. 2 Cs60Pb40 alloy cooling thermogram AU—liquid undercooled state, UR—recalescence, RB—cooling of the sample. The inset shows the dependence of the measured sample temperature at the completion of the recalescence process on the value of melt undercooling. The dots are experimental data; the line is the approximation equation that was used to extrapolate to zero undercooling
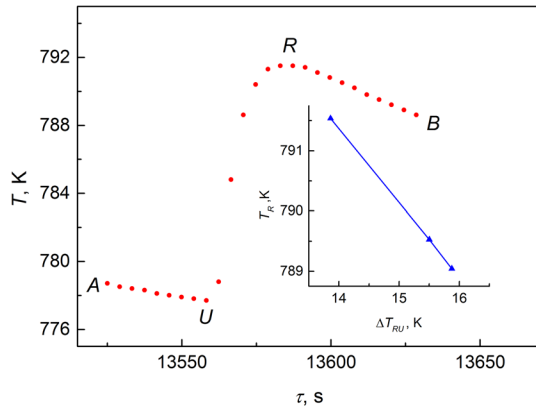
As estimated, the total standard uncertainty (Type B) of the obtained enthalpy data does not exceed 0.3%. The declared measurement accuracy was confirmed in experiments with leucosapphire, for which precision data on caloric properties are available [10]. A comparison of the results we obtained in [7] with the recommendations of [10] showed that in the range 575–1275 K, the deviation of the measured values from the reference values for enthalpy does not exceed 0.05% and for heat capacity—0.16%.

3 Results and Discussion

In Table 2, the results of thermal analysis of alloys are shown, and in Fig. 2, as an example, an experimental thermogram for the composition Cs60Pb40 is presented. In the case of significant undercooling relative to the liquidus temperature T_L or solid-phase transition T_t, the thermocouple readings at the end of recalescence (R in Fig. 2) were underestimated due to heat removal through its fittings. The true phase transformation temperature was found by linear approximation of the array $\left\{ T_R \left(\Delta T_{UR} \right) \right\}_i$ and subsequent extrapolation to zero undercooling. For

minor or zero undercooling, the T_R value was reproduced within 0.01…0.11 K and was taken as the true value of T_L or T_t.

Thermal analysis of the Cs50Pb50 alloy showed the existence of three thermal effects. Within the resulting measurement errors, the temperature of the onset of crystallization coincided with the data in [3, 6], where the values obtained were 920.6 ± 1.5 K and 920 ± 1 K, respectively. At the same time, according to [2], the liquidus temperature for this alloy is 893 ± 3 K, which indicates possible errors in the existing phase diagram of the cesium–lead system [2]. Another thermal effect is associated with the solid-phase transition. It was accompanied by significant undercooling, so the true temperature at which it occurs T_t was found by extrapolation to zero undercooling. Within the estimated errors, the value of T_t coincided with the transition temperature found in [6] (869 ± 1 K). In addition, another thermal effect was discovered, which was accompanied by a slight undercooling of 1.1–1.2 K. Its temperature is $T_1 = 902 \pm 3$ K. Unfortunately, at the moment it is not known what it is associated with.

When carrying out thermal analysis of the Cs33Pb67 alloy (66.67 at.% Pb), two thermal effects were fixed. The first corresponds to the onset of melt crystallization; the second is probably associated with the peritectic reaction [2]. For the compositions Cs40Pb60 and Cs60Pb40, the temperature of the onset of crystallization that we determined differs from the data in [3] by 0.3 K and 0.7 K, respectively. We emphasize that in [3] objective control was carried out to achieve homogeneity of melts, which is a necessary condition for obtaining reliable data on the properties of alloys in the liquid state and liquidus temperature. Good agreement in the T_L of the alloys in this work and [3] confirms our estimated temperature measurement errors and the absence of component concentration gradients in the melts.

In Table 3, the measured values of the molar enthalpy of the studied alloys $H_{298.15}(T) = M[h(T) - h(298.15K)]$ are presented, where T is the temperature, M is the molar mass, and h is the measured mass enthalpy. Since the temperature of the calorimetric block after dropping the ampoule differed from 298.15 K (for the experiments performed it varied within 295.4…307.8 K), then to determine $h(298.15$ K) the iterative procedure described in [9] was performed.

To apply the iterative procedure, it is necessary to know the enthalpy of the solid phase at low temperature. Since it is impossible to measure the low-temperature enthalpy of the Cs60Pb40 alloy in the solid phase (the sample crystallizes completely only at the melting point of cesium, i.e., about 301 K), a different method was used to reduce the enthalpy to a standard temperature. From the phase diagram [2] it follows that at 298.15 K the sample is a mixture of two solid phases—pure cesium and the Cs50Pb50 compound. This allows us to calculate the heat capacity of the Cs60Pb40 alloy at 25 °C according to the additivity rule using data on the heat capacity of solid cesium and Cs50Pb50 from [11] and this work, respectively.

The primary data (Fig. 3) were approximated using the least squares method with polynomials of the form:

Table 3 Results of alloy enthalpy measurements*

T, K	$H_{298.15}$, J/mol	T, K	$H_{298.15}$, J/mol
Cs33Pb67		Cs50Pb50	
430.8	3890		
450.6	4485	430.8	3516
470.3	5095	450.6	4042
490.3	5698	470.3	4573
510.3	6290	490.1	5104
530.1	6890	510.1	5650
728.5	13,276	529.9	6193
803.0	15,759	549.7	6732
851.8	26,658	629.1	8944
876.8	27,832	678.8	10,360
926.3	29,882	728.2	11,802
976.0	31,799	778.1	13,306
1025.8	33,631	827.5	14,852
1075.6	35,393	857.6	15,801
1075.7	35,459	872.2	22,381
1075.8	35,407	886.6	23,005
1075.9	35,463	886.9	23,009
Cs40Pb60		896.7	23,500
431.2	3893	926.5	28,963
450.9	4506	931.3	29,323
470.6	5110	946.2	30,474
490.4	5732	976.0	32,576
510.3	6382	1000.8	34,278
530.0	7037	1026.0	35,864
887.2	26,954	1050.8	37,280
906.6	27,959	1076.1	38,706
926.5	28,927	1076.2	38,639
951.6	30,096	1126.1	41,119
976.4	31,234	1176.5	43,203
1001.4	32,279	Cs60Pb40	
1002.3	32,341	827.6	23,488
1026.4	33,386	827.7	23,575
1051.5	34,326	852.0	24,640
1076.0	35,331	901.9	26,894
		951.6	29,247
		1001.3	31,667
		1051.4	33,925
		1076.3	35,143
		1076.4	35,137

*No correction to the enthalpy for condensation of cesium vapor in the ampoule was introduced because the assessment showed (according to the ideal solution laws) that its value at the maximum measurement temperature does not exceed 0.07–0.12%, which is significantly less than the estimated measurement errors. Strong interaction between components in melts of the cesium–lead system further reduces the actual contribution from condensation
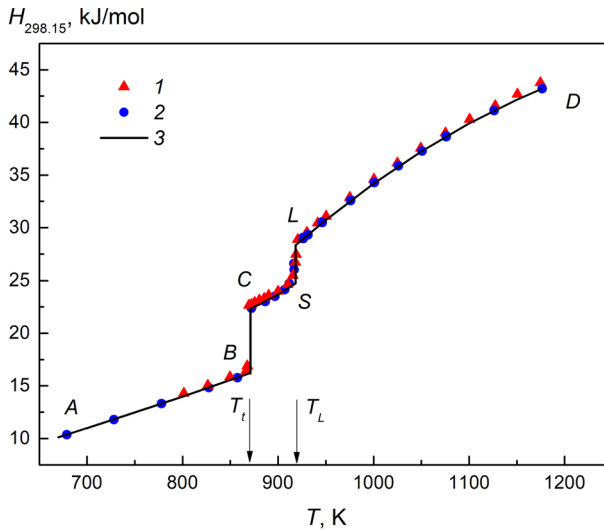
Fig. 3 Enthalpy of Cs50Pb50 alloy in solid and liquid states. *1*—measurement results of [6], *2*—experimental data of this work, *3*—calculation using approximation equations (Table 4)

$$H_{298.15}(T) = \sum_{i=0}^{k} A_i (T - T_0)^i. \tag{1}$$

The data approximation for the low-temperature solid phase was carried out with the additional condition $A_0 = 0$, $T_0 = 298.15$ K. The optimal degree of k was chosen based on the analysis of the experimental heat capacity (Fig. 4)

$$C_p^i(T_j) = \frac{H_{298.15}^{i+1} - H_{298.15}^{i-1}}{T_{i+1} - T_{i-1}}, \tag{2}$$

where i is the number of the experimental point, $T_j = \frac{T_{i+1} + T_{i-1}}{2}$, $H_{298.15}^i$ is the measured enthalpy value at temperature T_i. It should be noted that the type of function for approximating measurement results in the mixing method is important, because the heat capacity is found by differentiating the smoothed enthalpy data. An unjustified choice of the form of the approximation equation can lead to significant errors in determining the heat capacity and to nonphysical anomalies in the $C_p(T)$ dependence. Table 4 shows the results of processing the experiments.

Figures 3 and 4 compare the obtained data on the caloric properties of the Cs50Pb50 alloy with the measurement results of [6]. It is worth noting that article [6] does not indicate the error in determining enthalpy and heat capacity, and also does not provide the recommended temperature dependences of caloric properties. The authors presented only the initial experimental data, the form of the approximation equation without indicating the numerical values of its coefficients, as well as changes in enthalpy on phase transformations without indicating the method of their

Table 4 Experiment processing results*

	Phase	Cs33Pb67	Cs40Pb60	Cs50Pb50	Cs60Pb40
ΔT, K	Liquid	852–1079	887–1076	926–1177	827–1076
N		9	10	11	9
T_0, K		839	876.7	913.3	802
A_0, J/mol		26,135	26,441	28,338	22,301
A_1, J/(mol K)		44.53	51.35	78.26	46.74
A_2, J/(mol K^2)		− 0.0224	− 0.03445	− 0.08037	0
AAD, %		0.1	0.06	0.06	0.13
$\varphi(C_p)$, %		0.8–3.6	0.6–2.7	0.38–2.2	0.72
					Cs50Pb50
ΔT, K	Solid	431–530	431–530	431–857	872–897
N		8	6	13	4
T_0, K		298.15	298.15	298.15	871
A_0, J/mol		0	0	0	22,335
A_1, J/(mol K)		28.603	27.78	26.507	38.87
A_2, J/(mol K^2)		0.005178	0.01093	− 7.987 × 10^{-4}	0.2477
A_3 J/(mol K^3)		0	0	6.991 × 10^{-6}	0
AAD, %		0.16	0.14	0.05	0.01
$\varphi(C_p)$, %		0.7–1.4	1.0–3.3	0.1–0.4	2–5.5

*ΔT—temperature range in which experimental data were obtained; N—number of experimental points in the interval ΔT; $\varphi(C_p)$—uncertainty (type A) at 0.95 confidence level with a coverage factor of k = 2.

$AAD = \frac{1}{N} \sum\limits_{i=1}^{i=N} \left| \frac{H_{298.15}^i - H_{298.15}(T_i)}{H_{298.15}(T_i)} \right|$, where $H_{298.15}(T_i)$—enthalpy calculated using the approximation equation at temperature T_i

Fig. 4 Heat capacity of Cs50Pb50 alloy in a liquid state. Dots—experimental heat capacity (calculation by Eq. 2), solid line—approximation equation (Table 4), dotted line—data [6]
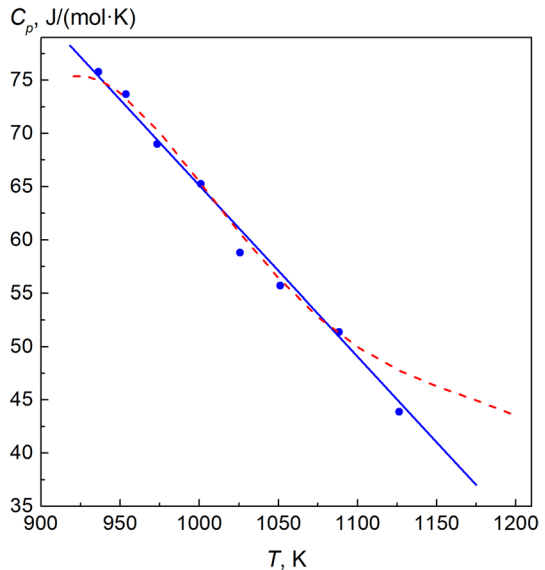
Fig. 5 Measured values of the heat capacity of Cs–Pb system melts (calculated by differentiating the smoothed enthalpy data). *1*—Cs33Pb67, *2*—Cs40Pb60, *3*—Cs50Pb50, *4*—Cs60Pb40. The uncertainty in determining the heat capacity of each alloy is given in Table 4
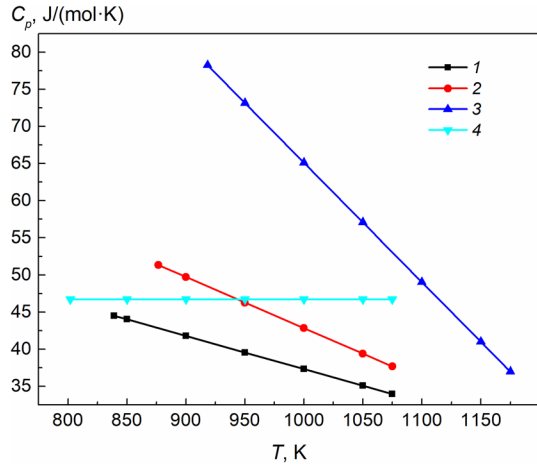

calculation. Data in Fig. 4 were obtained based on our approximation of the measurement results [6] with the dependence $H_{298.15}$ (T) recommended in that work. It is clear from the figures that the enthalpy of solid phases in [6] throughout the entire temperature range of their existence (excluding regions adjacent to the temperature of solid-phase transformation) systematically exceeds our data by the same value equal to 1.7%. This, in particular, indicates good agreement between the data on the enthalpy change on solid-phase transition, although the difference exceeds the total error in enthalpy determination. More significant deviations near the solidus and T_t are most likely associated with the onset of melting of the samples and the transition to the high-temperature phase. The measured enthalpy [6] of the melt up to 1125 K also exceeds our data by a constant value of about 1%, and only at higher temperatures the deviation increases to 1.8% at 1175 K.

As one would expect from the above, the heat capacity of the liquid alloy in our work and in [6] from liquidus to 1100 K are in excellent agreement with each other, although at the maximum measurement temperature the difference increases to 20%, which significantly exceeds the estimated errors of our measurements.

In Figs. 5, 6 and 7, the temperature and concentration dependences of the heat capacity of the studied alloys in the liquid state are presented. It can be seen that for all alloys except Cs60Pb40, the heat capacity decreases with increasing temperature, and its absolute value reaches the maximum at a concentration of about 50 at. % lead. Using data on the heat capacity of pure cesium and lead [11, 12], we compared the temperature dependences of the heat capacity of liquid Cs–Pb system alloys that we obtained with the values calculated using the additivity rule for the ideal solution. It turned out that the deviation of the measured C_p from additive values reaches enormous values: up to 165% for equiatomic composition (Fig. 6). A significant deviation from additivity of such properties as heat capacity and molar volume is abnormal for typical liquid metal systems [13, 14].

The position of the maximum of the heat capacity coincides with the position of the peaks on the concentration dependences of other structure-sensitive properties of this system [2, 3]. This, as well as a significant deviation of C_p from additive values,

Fig. 6 Relative deviations of the measured values of the heat capacity of Cs–Pb system melts from calculations based on the additivity rule for the ideal solution. *1*—Cs33Pb67, *2*—Cs40Pb60, *3*—Cs50Pb50, *4*—Cs60Pb40. $\delta C_p = \frac{C_p - C_p^{id}}{C_p^{id}}$, where C_p^{id} —heat capacity of the ideal solution
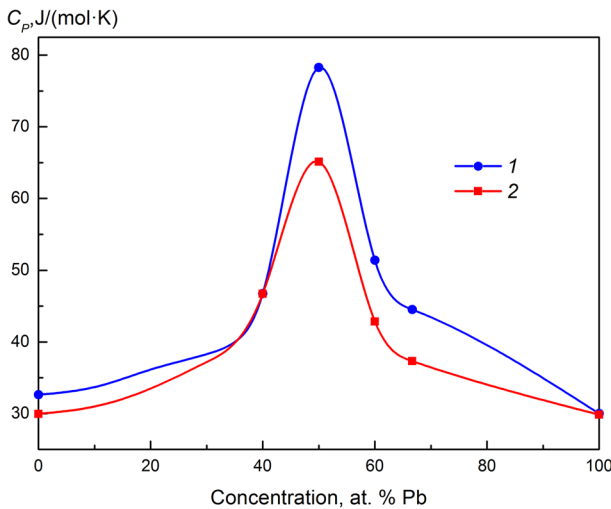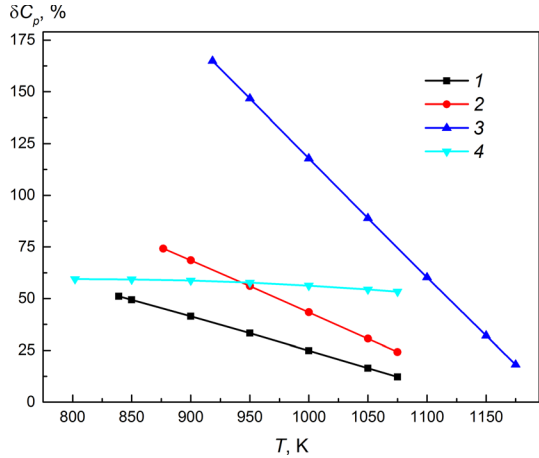
Fig. 7 Concentration dependence of the heat capacity of liquid Cs–Pb alloys at the liquidus temperature (*1*) and at 1000 K (*2*). The dots are data from this work. Lines—interpolation of points using cubic splines

confirms the assumption made by the authors [2, 4–6] about the structure of these melts, according to which in the liquid Cs–Pb system there is a tendency to develop complexes in the form of Pb^{-4} tetrahedra surrounded by cesium cations, and the concentration of such complexes reaches its maximum near the liquidus temperature and at a content of about 50 at.%. Pb. As the temperature increases, it is assumed that the concentration of ionic complexes decreases due to their dissociation, which smooths the maximum in the concentration dependence of the heat capacity. The decomposition of ionic complexes also explains the decrease in the heat capacity of melts of the cesium–lead system with increasing temperature.

4 Conclusion

New reliable experimental data have been obtained on the enthalpy and heat capacity of four alloys of the Cs–Pb system containing 40, 50, 60, and 66.7 at.% Pb in a wide temperature range, including solid and liquid states. Data on the caloric properties of alloys other than Cs50Pb50 are obtained for the first time and currently remain the only ones. The change in enthalpy of alloys during melting and solid-phase transitions is determined. A comparison with the available literature data on the caloric properties of the alloy of equiatomic composition shows good agreement of the results. It is demonstrated that the existing phase diagram of the cesium–lead system contains inaccuracies and requires additional research. The experimental data obtained indirectly confirm the existing ideas that the structure of melts of the Cs–Pb system has complexes of the Cs_4Pb_4 type, the concentration of which decreases with increasing temperature. The obtained results contribute to the experimental database for the development of the theory of ion-metal melts.

Data Availability All data generated or analyzed during this study are included in this article.

Declarations

Conflict of interest The authors declare that they have no conflict of interest.

References

1. V.F. Gantmakher, Usp. Fiz. Nauk (2002). https://doi.org/10.1070/PU2002v045n11ABEH001246
2. J.A. Meijer, G.J.B. Vinke, W. van der Lugt, J. Phys. F: Met. Phys. (1986). https://doi.org/10.1088/0305-4608/16/7/012
3. R.A. Khairulin, R.N. Abdullaev, S.V. Stankus, Phys. Chem. Liq. (2021). https://doi.org/10.1080/00319104.2020.1793335
4. H.T.J. Reijers et al., Phys. Rev. B (1989). https://doi.org/10.1103/PhysRevB.40.6018
5. H.T.J. Reijers, W. van Der Lugt, M.L. Saboungi, Phys. Rev. B (1990). https://doi.org/10.1103/PhysRevB.42.3395
6. M.L. Saboungi et al., J. Chem. Phys. (1988). https://doi.org/10.1063/1.455538
7. S.V. Stankus, I.V. Savchenko, O.S. Yatsuk, Instrum. Exp. Tech. (2017). https://doi.org/10.1134/S0020441217030265
8. S.V. Stankus, I.V. Savchenko, O.S. Yatsuk, High Temp. (2018). https://doi.org/10.1134/S0018151X18010170
9. S.V. Stankus, I.V. Savchenko, O.S. Yatsuk, E.P. Raschektaeva, Russ. J. Phys. Chem. A (2018). https://doi.org/10.1134/S0036024418090285
10. D.A. Ditmars, T.B. Douglas, J. Res. Natl. Bur. Stand., Sect. A (1971) https://doi.org/10.6028/jres.075A.031
11. L.V. Gurvich et al, Thermodynamic Properties of Pure Substances. Handbook: Vol. 4. Book 2 (Nauka, Moscow, USSR, 1982) [in Russian]

12. P.H. Sommelet, Gibbs Energies, Entropies and Heats of Formation from Drop Calorimetry: the Silver Lead System: M.S. Thesis (Berkley University, 1965)
13. R.N. Abdullaev, R.A. Khairulin, Y.M. Kozlovskii et al., Int. J. Thermophys. (2023). https://doi.org/10.1007/s10765-023-03187-1
14. M.H. Buschmann, Int. J. Thermophys. (2024). https://doi.org/10.1007/s10765-023-03295-y